International Journal of Heat and Mass Transfer 116 (2018) 1085–1095

Contents lists available at ScienceDirect

International Journal of Heat and Mass Transfer

journal homepage: www.elsevier.com/locate/ijhmt

Experimental study on heat transfer and pressure drop characteristics of fin-and-tube surface with four convex-strips around each tube

Xiao-Yu Li, Zhao-Hui Li, Wen-Quan Tao *

Key Laboratory of Thermo-Fluid Science and Engineering of MOE, Xi'an Jiaotong University, Xi'an, Shaanxi 710049, China

ARTICLE INFO

Article history:
Received 1 June 2017
Received in revised form 17 August 2017
Accepted 19 September 2017
Available online 4 October 2017

Keywords:
Heat transfer enhancement
Pressure drop
Convex fin
Experimental correlation
Air cooler

ABSTRACT

In the present study, heat transfer and friction characteristics of heat transfer exchanger with a new type of enhanced fin – convex fin was experimentally investigated. For comparison, a plain-fin heat transfer surface with the same dimension was also tested. At low Reynolds number the airside convective heat transfer coefficient of the convex-fin is 25% higher than that of the plain-fin. At high Reynolds number the heat transfer coefficients of the convex-fin is slightly higher than the heat transfer coefficient of the plain fin. The pressure drop of the new enhanced fin increases by 16%. The convex-fin is suitable for enhancing heat transfer at low and middle velocity condition commonly encountered in air-cooling industry.

1. Introduction

Finned tube heat exchangers have been widely used in various engineering fields such as heating, ventilation, air conditioning and refrigeration (HVAC&R) systems. In an air-cooling fin-and-tube heat exchanger, heat transfers from the air flowing outside tubes to the liquid flowing inside the tubes. Because the heat transfer capability of air is very poor due to its low thermal conductivity and density, over 90% of the total thermal resistance from air to liquid lies on the air side. Therefore a series of fin-surfaces have been developed. Broadly speaking, they can be classified into following four groups, namely, (1) plain plate fin; (2) wave fin; (3) interrupted fin, including strip fin and louvered fin and (4) fin with vortex generators. A brief review of these four kinds of fins is given below.

A lot of studies, both experimental and numerical, have been conducted on the air heat transfer and pressure drop performance for the above-mentioned types of fin-and-tube surfaces. References examples include: [1–3] for plain plate fin, [4–7] for wavy-fin, [8–19] for interrupted fin and [20–26] for fin with vortex generators. Wang et al [1] performed experimental studies on the air side performance on 18 samples with plain fin configurations and found out the effect of fin pitch, tube rows and tube diameter on heat transfer and friction characteristics. Then in Reference [2] Wang and co-workers used the data of 74 samples to develop a correlation for fin-and-tube heat exchanger with plain fin. The correlation can predict more than 85% experimental data with the deviation less than 15%. He et al. [3] performed numerical investigation for plate fin-and-tube heat exchanger. Five parameters including Reynolds number, fin pitch, longitudinal tube pitch, spanwise tube pitch and tube row number were examined. The results were analyzed and well described from the view point of field synergy principle. Wang et al. [4] also performed a series of extensive experiments on pressure drop and heat transfer of wavy fin-and-tube heat exchangers. Eighteen samples with different parameters were measured. The result shows that the heat transfer characteristics are independent of fin pitch; the number of tube row has negligible effect on friction factors and the heat transfer coefficients for wavy fin are 55% to 70% higher than that of plain fin. Tao [5–7] and co-workers performed a series of numerical simulation of heat exchangers with wavy fin surface. In Reference [5] numerical studies for wavy fin heat exchanger with two different shapes of tubes (circular and elliptic) were carried out. The result shows that the heat transfer coefficient of elliptic tubes is increased by 30% and the increase of friction factor is only 10%. In [6] the prediction results of Nusselt number, friction factor and fin efficiency calculated by numerical simulation were compared with two experimental correlations. They found that the fin efficiency of wavy fin is larger than that of plain fin and with the increase of *Re* the effects of wavy angle are more and more significant. In [7] the authors examined the effect of four different parameters including Reynolds number, fin pitch, tube row number and wavy angle. The result shows that *Re* and wavy angles have

* Corresponding author.
E-mail address: wqtao@mail.xjtu.edu.cn (W.-Q. Tao).

https://doi.org/10.1016/j.ijheatmasstransfer.2017.09.076
0017-9310/

Nomenclature

A	heat transfer area (m^2)
A_c	minimum free-flow area (m^2)
D_c	tube diameter, including fin collar thickness (m)
D_h	$4A_cL/A$, hydraulic diameter (m)
F_f, F_j	enhance factor
F_p	fin pitch (m)
f	friction factor
G	mass flow rate (kg/s)
g	gravity (m/s^2)
H	effective tube height (m)
h	heat transfer coefficient (W/m^2 K)
h_{fg}	latent heat (kJ/kg)
j	the Colburn factor
k	overall heat transfer coefficient (W/m^2 K)
L	depth of the heat exchanger (m)
P_l	longitudinal tube pitch (m)
P_t	transverse tube pitch (m)
r	radius of the tube
R	thermal resistance (K/W)
S_S	breadth of a slit in the direction of airflow (m)
S_W	width of slit (m)
T	temperature (°C)
t	time (s)
u_m	maximum velocity (m/s)
V	volume (m^3)
X_L	$\sqrt{(P_t/2)^2 + P_l^2}/2$ geometric parameter (m)
X_M	$P_t/2$ geometric parameter (m)

Greek symbols

Δp	pressure drop (Pa)
δ	thickness (m)
η	fin efficiency
η_o	surface efficiency
λ	thermal conductivity (W/m K)
μ	dynamic viscosity (kg/m s)
ν	kinematic viscosity (m^2/s)
ρ	density (kg/m^3)
σ	contraction ratio of cross-sectional area
Φ	heat transfer rate (W)

Subscripts

a	air
c	convex fin
cor	by correlation
exp	by experiment
f	fin
i	tubeside
in	airside inlet
m	mean
o	airside
out	airside outlet
p	plain-fin
t	tube
w	water

positive effect on heat transfer and the other two factors have negative effect. All these results are agreeable very well with the field synergy principle. The first study related to slit fin was conducted by Nakayama and Xu [8]. They presented test results for three samples, and proposed a correlation based on these results. After 1999 lots of works on interrupted fin surface have been presented. Wang et al. [9] tested as many as 49 samples of louvered fin-and-tube heat exchangers and developed the correlations for louvered fin. Yun and Lee [10] investigated the performance of interrupted surfaces of multi-tube row with different shape and recommended an optimal fin shape for air conditioners. Kang and Kim [11] found that under the same fan power hybrid fin with strips at fin sheet of rear row are more effective than that with strips at whole fin sheet. Lozza and Merlo [12] performed experimental investigation on different kinds of fin surface including plain fin, wavy fin, louvered fin and winglet fin. Their experiments show that louvered fins provide the best heat exchanger performance. Cheng et al. [13] performed a numerical investigation on four types of plain and strip fin surfaces. The results show that among three types of strip fin designed by "front sparse and rear dense", the fin which behaves the best has the least synergy angle between velocity and fluid temperature gradient. Qu et al. [14] also performed a numerical computation on four types of strip fin surfaces and their results show that enhancement structures placed in the rear part of the fin can be more effective compared with that placed in the frontal part. Zhou and Tao [15] found that at the same frontal velocity the full slotted fin surface have the highest heat transfer rate but at the identical pumping power the slotted fin surface with strips mainly located in the rear part behaves the best. Jin et al. [16,17] first discussed in the literature the convergence criteria of numerical simulation for fin-and-tube structures and observed the turning *Re* number below which slotted fin performs worse than plain fin. Tao et al. [18] studied five types of slit fins and concluded that the slit fin has the best heat transfer performance when the thermal resistance is uniformly distributed. Kim and Cho [19] experimentally investigated on slit fin and plain fin heat exchangers with 5.3 mm tube diameter. Results reveal that slit fin has higher *j* factor and *j/f* ratio. Fiebig et al. [20] performed experiments to investigate the effect of wing-type vortex generators on the performance of heat exchanger. Fin with a pair of vortex generators behind each tube can increase the heat transfer by 55–65% and pressure drop by 20–45%. In 1995, Jacobi and Shah [21] reviewed the previous works of vortex generators and indicated that a deeper understanding of the flow and heat transfer interactions is needed to identify promising implementations for specific applications. Joardar and Jacobi [22] numerically studied the flow and heat transfer characteristics for surface enhanced by an array of delta-winglet vortex generators. Their investigation show that the winglet vortex generators significantly enhance the local heat transfer on the downstream tube and fin surface and 3 vortex generators inline arrangement structure can enhance the heat transfer by 32% with the pressure drop increase by the same scale. Wu and Tao [23] reveal that the heat transfer enhancement mechanism of the longitudinal vortex generator is the improvement of synergy between velocity and fluid temperature gradient. They also found that the attack angle of 45 °has better enhancement effect compared with the attack angle of 30°. Tian et al. [24] compared the performance of fin with rectangular and delta winglet pair. There are two main conclusions in their study: the first is that the delta winglet pair has better performance; the second is that for rectangular winglet pair the common-flow-down configuration has a better performance than that of common-flow-up. He and Zhang [25] summarized the papers from 1990s to 2000s in the study on vortex generator techniques. They conclude that further investigation should be focus on finding out the best arrangement of the vortex generators for different heat exchangers. Li et al. [26] proposed a new kind of plain fin with twelve winglets arranged around each tube. Their numerical simulation proved that the proposed fin

has better comprehensive performance compared with wavy fin and a five- row structure with such located LGVs could have the same heat transfer rate of that of six row wavy fin-and-tube structure.

Although so many efforts have been paid on air-side enhanced heat transfer technology as briefly mentioned above, most of these studies are concentrated on tube outside diameter smaller than 10 mm and tube row number less than 6 which are usually applied in air conditioning engineering. For air-cooler tube used in air compressor cooling technology the outer diameters are usually around 20 mm and the tube row number often larger than 10. Whether the correlations proposed in the above-mentioned references can be applied still needs to be examined. On the other hand, pressure drop is always one of the main problems that researchers have to face with in enhanced heat transfer studies. Especially for the mid-cooler between air compressors, pressure drop is a crucial factor for the entire compressor system. Another problem for applying the enhanced heat transfer technology is that condensate water formed in the cooling process may clog the enhancing structure. For compressed air with high temperature and pressure, large amount of condensate water will be separated out in the downstream part of the air-cooler and many of the enhanced technique can't be adopted in such condition. Especially for surfaces with slotted fin having its mouth normal to flow direction the water condensate may easily blocks the slit, leading to a sharp increase in pressure drop and deterioration in heat transfer.

In order to adapt the aforementioned situation of air cooler used in compressor a new kind of fin-and-tube surface with four convex-strips around each tube was adopted in some air-cooler products made in China as shown in Fig. 1. For this new fin-and-tube structure there are three advantages described below. First engineering practice has shown that the convex-strip induced pressure drop penalty is relatively low; second the mouths of the four convex strips are around each tube hence they have better resistance to the blockage by condensate water compared with those slotted fin whose mouths are normal to the main flow direction; third, the convex structure of the fin can enhance the mechanical strength of fin sheet which is useful from the manufacture point of view. However, to the author' knowledge, no public information can be found in the literatures about the heat transfer and friction factors of this structure. In this paper, this new surface is experimentally investigated under the frontal dry air velocity varies from 2.5 m/s to 9 m/s, which covers the velocity range usually adopted in the air-cooler design. For comparison, a plain-fin heat exchanger having the same sizes is also tested at the same velocity range.

In the following presentation, test facility and procedure will be presented in Section 2, followed by the data reduction method in Section 3.Then test results will be presented and discussed in Section 4, and finally some conclusions will be drawn in Section 5.

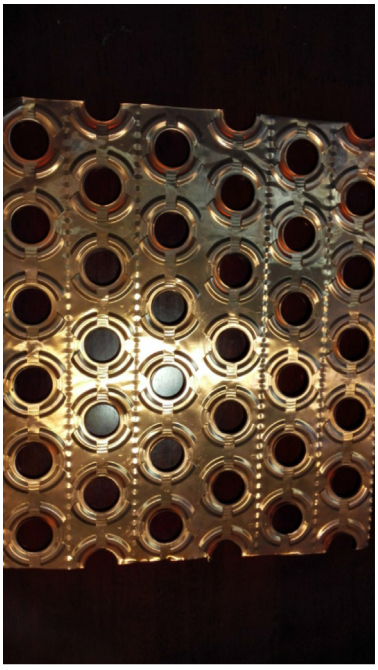

(a) Top view of the fin tested

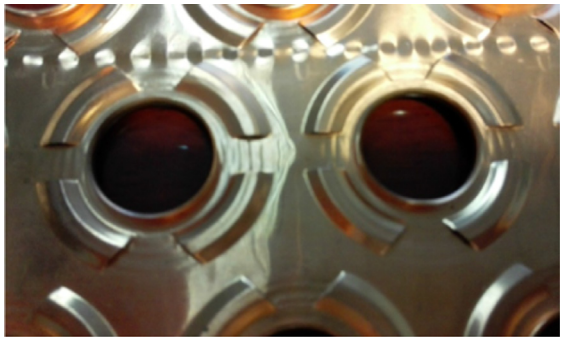

(b) Magnified picture of the four convex-strips around tube

Fig. 1. Tested fin structure.

2. Experimental apparatus and experimental procedure

Three heat exchanger samples are tested in this study: a smooth tube heat exchanger, a plain-fin-and-tube heat exchanger, and a convex-fin-and-tube heat exchanger. The first one is used for verify the test system, and the second one is adopted for the comparison with the 3rd one. Both the tubes and the fins of the test samples are made of copper. In compressor air cooler the copper (rather than aluminum) fin is used because of much larger air velocity is used compared with that in air-conditioning and copper fin sheet has a stronger mechanical strength than that of aluminum. All three specimens have the same geometrical dimensions. The samples have the frontal and dorsal area of $250 \times 300 mm^2$. The samples have twelve rows of tube in the air flow direction. The arrangement of tube bank is staggered, and there are six tubes in odd row and five tubes in even row. The side and top view of the tested heat exchanger is shown in Fig. 2. The dimensions of the fin surface with convex-strips are shown in Fig. 3, and the major geometric dimensions are listed in Table 1.

Fig. 4 is the schematic diagram of the test apparatus. Fig. 5 is photos of experiment apparatus and test heat exchanger. The induced wind tunnel used in the test consists of two circuits, an air circuit and a steam condensation circuit. Air from the room goes in the inlet with the size of cross section area of $1250 \times 930 mm^2$, then it passes through the transition section, contraction section and stabilization section in turn until reaching the test section. Air flows through the tube bank perpendicularly. Inner the tube water vapor condensation occurs and the latent heat transfers to the air flowing through tubes and fins. Heated air leaving the test section passes through a velocity measurement section before being released into atmosphere by a draught fan. The steam is generated by an electric boiler which has three 8 kW electric heaters and three 16 kW electric heaters. The power of the boiler can be adjusted by a transformer. The vapor condenses at a pressure a bit higher than the atmosphere and is a bit overheated by a superheater before it goes into the top head of the heat exchanger where

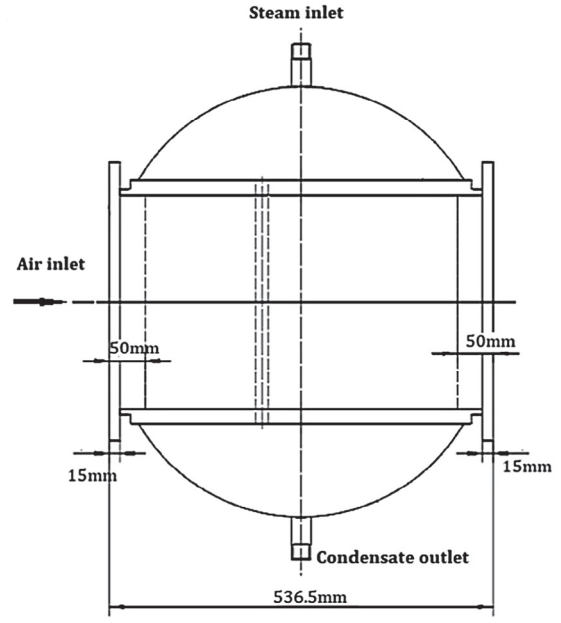

(a) Side view of the tested heat exchanger

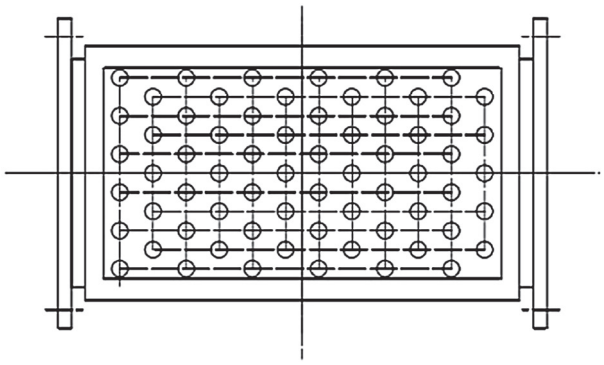

(b) Top view with the head being moved

Fig. 2. Outlines of tested heat exchanger.

it's distributed into different tubes. The condensate water flows into a volumetric flow meter and back to the boiler ultimately.

The inlet and outlet air temperatures are measured with two sets of thermo-electric piles each is composed of sixteen pairs of copper constantan thermocouples. The junctions are connected in series and the arithmetic summation of the potential of each thermocouple represents the average temperature of the air flow. The electric potential of thermo-electric pile is measured with Keithley 2700 + 7708 card.

The average air speed is measured by a Pitot tube at velocity measurement section of the wind tunnel. Pitot tube has been demarcated before test. Dynamic pressure and static pressure are measured by U-shaped differential gage and YYT-200B tilted micro manometer, respectively. Before test, cross section speed distribution at velocity measurement section has been measured. The relation between the maximum wind velocity and cross section average wind velocity has been determined. In test, Pitot tube is installed in the center of tunnel to measure the maximum wind velocity, which is then converted to average wind velocity through demarcated relation. Flow resistance through tube bundle is measured by a U-shaped tube differential gage through static vents on four sides at two cross sections in front of and behind test specimen of the wind tunnel.

The saturation temperature of the steam is determined by steam pressure which is measured by mercurial U-shaped differential gage before the test section. Through regulating electric heater's power, saturated steam pressure is kept stable. During the test of one data run, it is allowed to fluctuate about 3–5 mm Hg (the steam gage pressure is about 200 mmHg). By controlling this vapor pressure the temperature of the vapor remains almost constant through the test process of one data run. The condensate flow rate is calculated by measuring the time that condensate water fills a fixed volume container (200 cm^3). For a fixed test case when the fluctuation of outlet air temperature is within 0.2 °C, the experiment is regarded to reach steady state, and then the experimental data are recorded. The averaged values of three measurements are taken as the test data for one case. The heat transfer rate is measured from both air side and condensate side, and their unbalance should be less than 5 % (except the air velocity or the heat transfer rate is very low). The average heat transfer rate of air side and condensate side is used to determine the overall heat transfer coefficient of the tested heat exchanger.

3. Data reduction and uncertainty analysis

Relationship between the overall thermal resistance and partial thermal resistance, which are based on the air side total heat transfer area (A_o) of the test specimen, is shown as follows [27]:

$$\frac{1}{k}=\frac{1}{h_i}\cdot\frac{A_o}{A_i}+\frac{1}{h_o\eta_o}+\frac{\delta}{\lambda}\cdot\frac{A_o}{A_i} \tag{1}$$

where δ and λ are the tube wall thickness and the tube wall thermal conductivity.

The overall heat transfer coefficient k is determined by

$$k=\frac{\Phi_m}{A_o\Delta T_m} \tag{2}$$

where ΔT_m is the logarithmic mean temperature difference defined by

$$\Delta T_m=\frac{T_{out}-T_{in}}{ln\frac{T_{out}-T_w}{T_{in}-T_w}} \tag{3}$$

T_w is the condensed water temperature inside the tubes. It is equal to the saturation temperature of water vapor.

The overall surface efficiency η_o is

$$\eta_o=1-\frac{A_f}{A_o}(1-\eta) \tag{4}$$

The fin efficiency η is calculated by the method proposed in [28]

$$\eta=\frac{tanh(mr\varphi)}{mr\varphi} \tag{5}$$

where

$$m=\sqrt{\frac{2h_o}{\lambda_f\delta_f}} \tag{6}$$

$$\varphi=\left(\frac{R_{eq}}{r}-1\right)\left[1+0.35\ln\left(\frac{R_{eq}}{r}\right)\right] \tag{7}$$

$$\frac{R_{eq}}{r}=1.27\frac{X_M}{r}\left(\frac{X_L}{X_M}-0.3\right)^{0.5} \tag{8}$$

where r is the radius of the tube including fin collar thickness, λ_f and δ_f are the thermal conductivity and thickness of the fin and X_M and

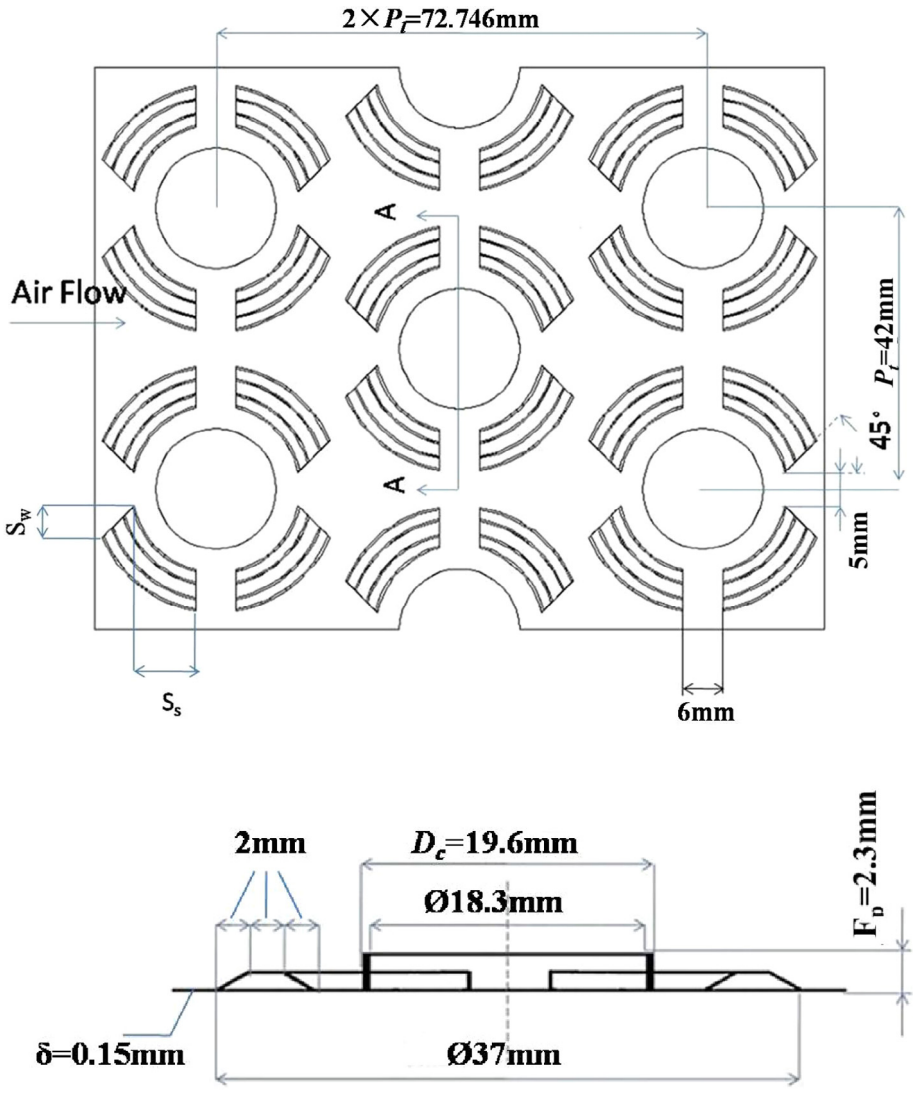

Fig. 3. Geometry of enhanced fin surface.

Table 1
Major parameters of the tested fin surface.

D_c (mm)	F_p (mm)	P_l (mm)	P_t (mm)	δ (mm)	S_w (mm)	S_s (mm)	Row No.
19.6	2.3	36.4	42	0.15	4.24	9.45	11

X_L are defined in the Nomenclature. R_{eq} is the equivalent radius defined in Eqs. (7) and (8).

The heat transfer coefficient inside the tubes, h_i, in Eq. (1) is determined by the Nusselt correlation:

$$h_i = 1.177\left(\frac{g\rho_w^2 h_{fg}\lambda_w^3}{\mu_g q H}\right)^{1/3} \tag{9}$$

the height of tubes, H, is equal to 0.3 m.

An iterative procedure based on Eqs. (5)–(8) is needed to get the airside heat transfer coefficient h_o and the surface efficiency η_o for a given measured k defined in Eq. (1).

The definitions of Reynolds number, Nusselt number, friction factor and j factor of air side are as follows:

$$Re = \frac{u_m D_c}{v_a} \tag{10}$$

$$Nu = \frac{h_o D_c}{\lambda_a} \tag{11}$$

$$j = \frac{Nu}{RePr^{1/3}} \tag{12}$$

$$f = \frac{A_c}{A_o}\frac{\rho_m}{\rho_{in}}\left[\frac{2\Delta P\rho_{in}}{(\rho_m V_m)^2} - (1+\sigma^2)\left(\frac{\rho_{in}}{\rho_{out}} - 1\right)\right] \tag{13}$$

where D_c is the outer diameter of tube in the smooth tube test specimen and in plain-fin or convex-fin heat exchanger it is the outer

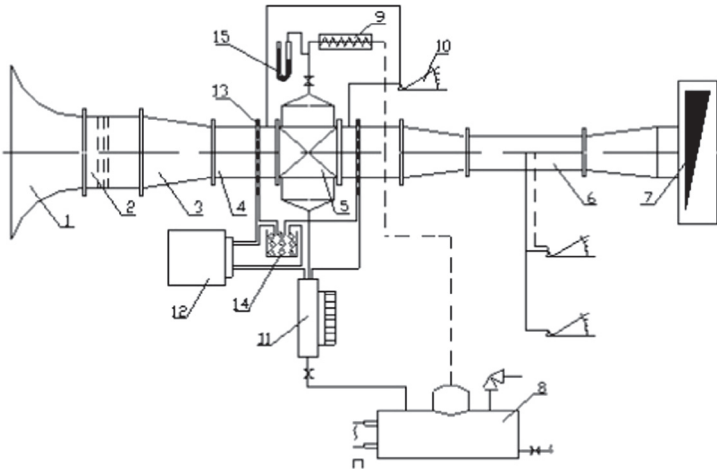

1 wind tunnel inlet; 2 transition section; 3 contraction section; 4 stabilization section; 5 specimen section; 6 velocity measurement section; 7 induced draught fan; 8 boiler; 9 superheater; 10 drag measurement; 11 volumetric flowmeter; 12 Keithley; 13 thermocouple; 14 ice bottle; 15 U-shaped tube

Fig. 4. Schematic of the experiment apparatus.

(a) Heat transfer wind tunnel without thermal insulation

(b) Cross section of test heat exchanger

Fig. 5. Experiment apparatus and test heat exchanger.

diameter of finned tube (i.e. the sum of the tube outer diameter plus two thicknesses of the fin). The air properties are determined by the arithmetic mean of air temperature at the inlet and outlet of the test section. The saturation temperature of steam is adopted to determine the condensate properties.

Table 2 lists the uncertainties of the measured parameters. With this information, the uncertainties of the data are analyzed by the method of Moffat [29,30].

From Eq. (2) we have:

$$\frac{\Delta k}{k} = \sqrt{\left(\frac{\Delta\phi}{\phi}\right)^2 + \left(\frac{\Delta A_o}{A_o}\right)^2 + \left(\frac{\Delta(\Delta T_m)}{\Delta T_m}\right)^2} \tag{14}$$

Uncertainty of heat transfer rate is about 5%, that of surface area about 1%. From the temperature measurement uncertainties (Table 2) and the difference of the outlet and inlet temperatures shown in the appendix, the maximum uncertainty of the logarithmic temperature difference is estimated 3%. Substitution of the above data into Eq. (14) yields: $\frac{\Delta k}{k} = 5.92$.

The uncertainty of the water vapor condensation heat transfer coefficient is difficult to obtain, since it was not directly measured, but separated from the total thermal resistance. However, according to [31–34] following estimation may be conducted. Eq. (1) can be rewritten in its thermal resistance form as follows:

$$R_{total} = R_i + R_o + R_w \tag{15}$$

The wall conduction resistance can be neglected, hence we have:

$$R_o = R_{total} - R_i \tag{16}$$

Table 2
Parameter ranges and uncertainties.

Parameter	Range	Uncertainties
Air temperature	10–110 °C	±0.1 °C
Frontal air velocity	1.98–8.52 m/s	±0.1 m/s
Air pressure drop	245–2479 Pa	±0.98 Pa
Vapor saturation temperature	106 °C	±0.6 °C
Time for condensate flow rate measurement	7–70 s	±0.05 s

where R_i is determined by Nusselt equation. It is widely accepted that Nusselt equation for condensation may have 10% uncertainty. Since the thermal resistance in vapor condensation-side accounts only for less than 5 percent of the overall thermal resistance, we can expect that the uncertainty of the air side heat transfer coefficient is similar to that of the total resistance, about 6 percent. The uncertainty of Reynolds number is estimated to be less than 5 percent and that of friction factor about 10 percent for the lowest velocity case.

4. Results and discussion

4.1. Experimental verification and experimental test

The reliability of the test system can be confirmed by comparing the experimental data of smooth tube specimen with Zhukauskas correlation [35]. The experimental relationship between *Nu* number and *Re* number of the smooth tube bank with 11 tube rows and the calculated result of Zhukauskas correlation is shown in Fig. 6. It can be seen that the experimental data agree with the Zhukauskas correlation very well and the differences between the predicted results and the experimental results are about 10%. The agreement between test data and correlation proves that the test system used in this study is reliable.

The relationship between Nusselt number and Reynolds number of convex-fin heat exchanger and plain-fin heat exchanger is shown in Fig. 7, where the black solid squares represent the data of the convex-fin test specimen and the red solid circles represent the data of the plain-fin test specimen. The black line is the correlation between *Nu* and *Re* of the convex fin and the red line is the correlation of the plain fin. The Nusselt numbers of the two heat transfer surfaces increase with the increase of *Re*. At low *Re* number (less than 7.5×10^3, which equals the frontal velocity less than 3.5 m/s); the Nusselt number of the convex-fin is significantly higher than that of the plain-fin. However, the enhancement effect of the convex-fin on heat transfer decreases with the increase of Reynolds number. In the test range of this study, the ratio of Nusselt number of the convex over plain samples varies from 1.2 to 1.05.

All the Nusselt number of the two tested surfaces are correlated individually as follows

For convex-fin:

$$Nu = 1.432Re^{0.422} (Re = 3500–15,000) \quad (17)$$

For plain-fin

$$Nu = 0.816Re^{0.475} (Re = 3500–15,000) \quad (18)$$

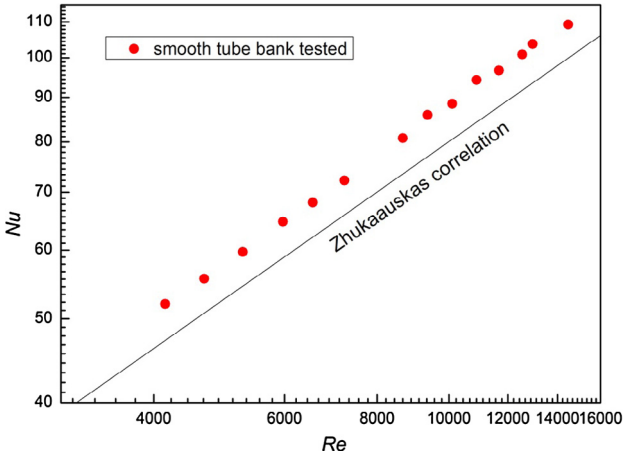

Fig. 6. Nusselt number vs. Reynolds number of smooth tube banks.

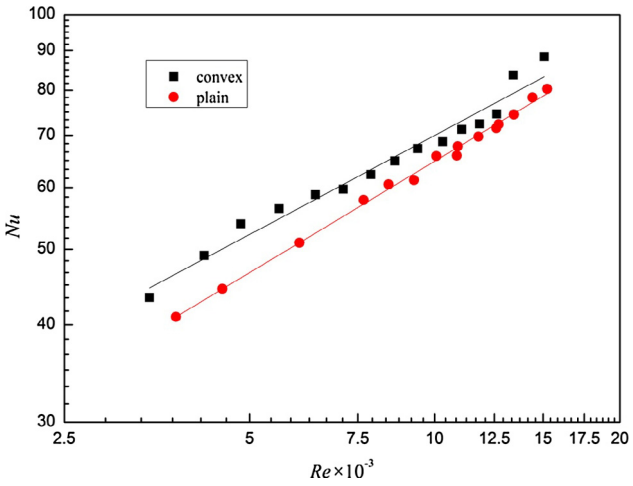

Fig. 7. Nusselt number vs. Reynolds number of convex and plain fin.

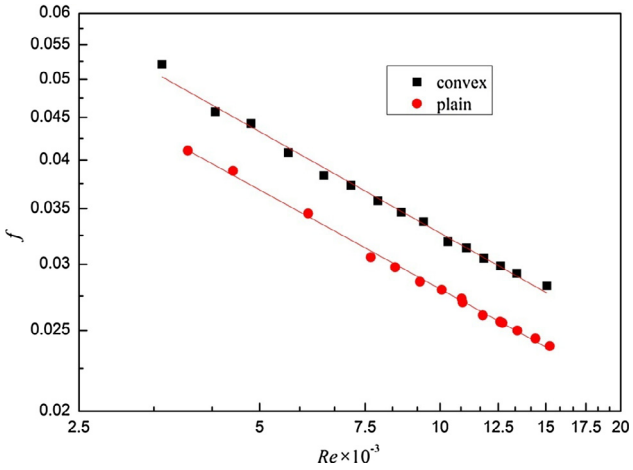

Fig. 8. Friction factor vs. Reynolds number of convex and plain fin.

The relationship between friction factor and Reynolds number of two samples is plotted in Fig. 8 which has the same legend as Fig. 7. It can be seen that the friction factor of convex fin is higher than that of the plain fin and both the friction factors decrease with the increase of *Re* number. At the same Reynolds number the friction factors of the convex-fin are about 16% higher than the plain-fin and the ratio is substantially retained in the test range. The correlated equations of the friction factor for tested fin surfaces are developed as below

For convex-fin:

$$f = 1.351Re^{-0.404} (Re = 3500–15,000) \quad (19)$$

For plain-fin:

$$f = 1.067Re^{-0.395} (Re = 3500–15,000) \quad (20)$$

For comparison and data accumulation of heat transfer community, our test data are included in the appendix of this paper.

4.2. Performance comparison and performance evaluation

As mentioned above, quite a few test results for similar geometries (but not exactly the same) have been published in literature. Therefore it is interested to compare our test results with them.

First the data of plain fin surface from this study are compared with the correlation developed by Wang et al. in Reference [2]. The values of P_t/D_c and P_l/D_c tested in this study are within the range of [2], and two major differences are tube diameter (19.9 mm vs. less than 10 mm) and tube row numbers (11 vs. less than or equal to 6). The comparison for j-factor and f-factor between correlations and experimental data are shown in Fig. 9 and Fig. 10, respectively. It can be seen that both the Colburn factor j and friction factor f predicted by their correlations agree with our experimental data very well with the maximum deviation of 15%. This results may imply that for the fin-and-tube surface the major factors influencing heat transfer and friction factor are its geometry and P_t/D_c and P_l/D_c, and the correlations proposed in [2] may be extended to cases with tube row number larger than 6. Of course this deduction should be further verified with more test data.

Second, we compare the results of our new convex fin (a kind of slit fin) with the investigation by Nakayama and Xu [8]. The geometries of the slit fin investigated by them are shown in Fig. 11.

According to Nakayama and Xu the j factor and f factor of slit fin can be expressed as follows:

$$j = j_p F_j \tag{21}$$

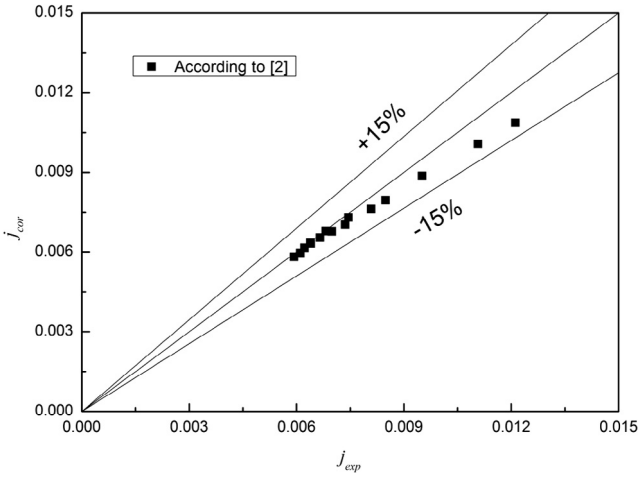

Fig. 9. J factor of the plain fin compared with correlation proposed by Wang [2].

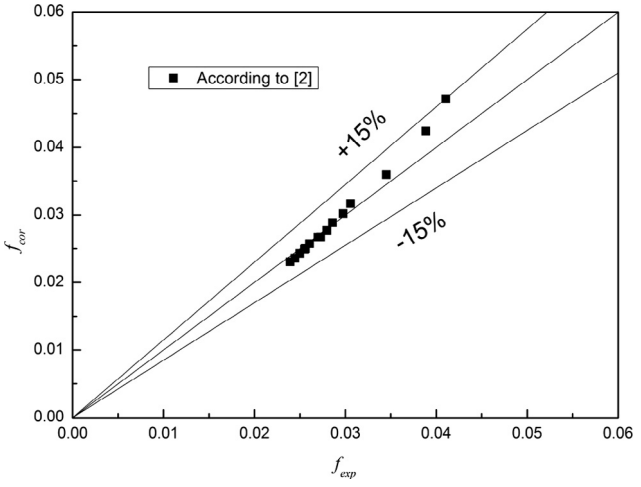

Fig. 10. F factor of plain fin compared with correlation proposed by Wang [2].

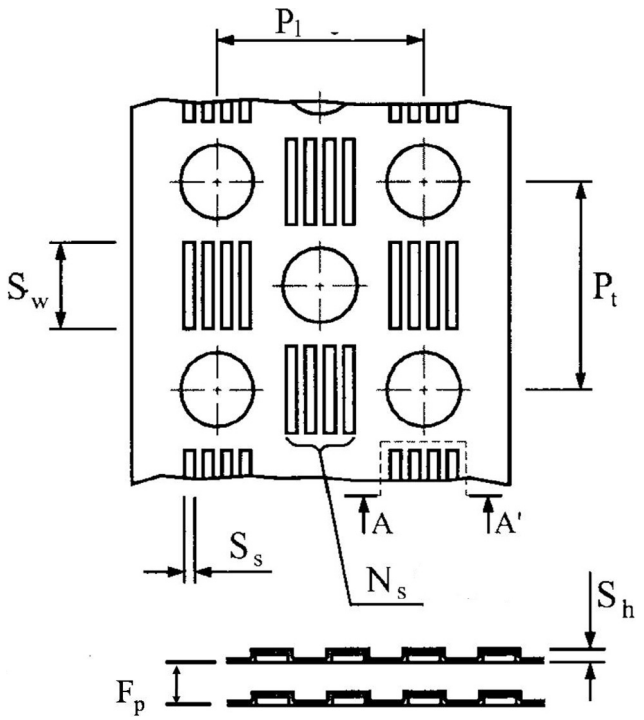

Fig. 11. Geometric parameters of slit fin proposed by Nakayama and Xu.

$$F_j = 1.0 + 1093\left(\frac{\delta_f}{F_p}\right)^{1.24}\phi_s^{0.944}Re_{D_h}^{-0.58} + 1.097\left(\frac{\delta_f}{F_p}\right)^{2.09}\phi_s^{2.26}Re_{D_h}^{0.88} \tag{22}$$

$$\phi_s = \frac{(2N_s - 1)S_S S_W}{P_t P_l - \frac{\pi D^2}{4}} \tag{23}$$

$$f = f_p F_f = f_p(1 + 0.0105Re_{Dh}^{0.575}) \tag{24}$$

where j_p and f_p are Colburn factor and friction factor of plain fin, respectively. F_j is the ratio of the j factor of the strip fin and that of the plain fin. F_f is the same ratio of the f factor. The definitions of N_s, P_l, P_t, F_p, S_s *and* S_w are shown in Fig. 11.

The convex fin surface studied in this paper is different from the traditional slit fin studied by Nakayama and Xu (Fig. 11), and the parameters of S_s and S_w need to be redefined. The other parameters, for example, the longitudinal tube pitch (P_l), transversal tube pitch (P_t) and fin pitch (F_p) are the same. The number of the slits (N_s) in the flow direction is equal to 2 for the studied surface. The new definitions of S_s and S_w are shown in Fig. 3. Under the same experimental condition, the ratio of the j factors of the two enhanced surfaces is equal to the ratio of Nusselt numbers. The factor F_j is calculated by dividing the Nu number of the convex (slit) fin got in the experiment by the Nusselt number of plain fin calculated by Eq. (18) under the same Re number. The calculation of F_f is similar with F_j. It turns out that F_j of the slit fin studied can be well predicted by Eqs. (22) and (23). The predicted F_j and our test data are compared in Fig. 12. The deviations between the predicted and tested F_j are all within a range of 5% while the deviations between predicted F_f and the experimental data are much larger as shown in Fig. 13. As mentioned above, at the same Reynolds number friction factors of the convex-fin are about 16% higher than that of the plain-fin in the test range, or in other words, F_f is around 1.16 in this study. It expressed by a dashed line in Fig. 13. The predicted value of F_f by Eq. (24) is much higher than our test results. The $F_{f\text{-}cor}$ is 20% higher than the $F_{f\text{-}exp}$ at low Re number and at high

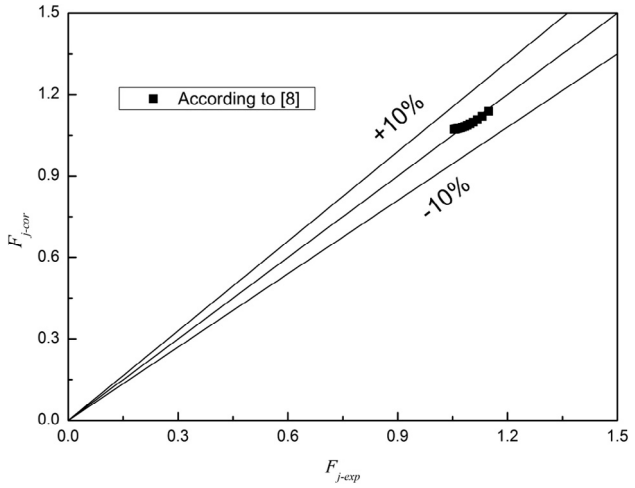

Fig. 12. F_j of *convex* fin compared with correlation proposed by Nakayama and Xu [8].

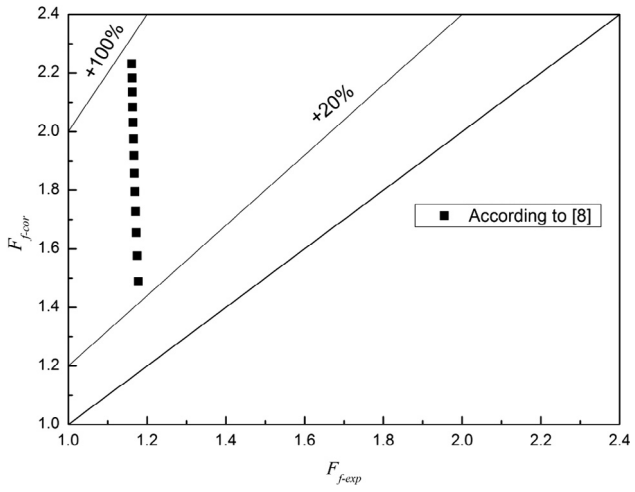

Fig. 13. F_f of convex fin compared with correlation proposed by Nakayama and Xu [8].

Re number the $F_{f\text{-}cor}$ is nearly double of $F_{f\text{-}exp}$. The superior heat transfer performance of the tested convex fin over the slit fin in [8] may be explained by the flow situation. In [8] the slit mouths are normally facing with the coming flow, causing larger pressure drop while enhancing the heat transfer. In the convex fin, when air passes through the convex domain in front of the tube, air is separated into four parts. Most of the air is uplifted by the convex and vortex is generated behind the convex. A part of the air flows into the mouth of the convex and flows through the convex. Some of the air flows straight to the tube and then flows between the tube and convex domain. These three situations can enhance heat transfer. The rest of the air passes between two convex domains. The convex domain behind the tube has one difference compared with the frontal one. The air flowing between tube and convex domain will be guided into the reversed flow area behind the tube and heat transfer can be significantly enhanced. The convex domains increase disturbance and pressure drop is increased as a result. The low pressure area behind the tubes is significantly reduced because more air flows into this area, making the pressure drop penalty of the convex fin being appreciably lower than that of slit fin in [8].

Thus we can draw a conclusion that the comprehensive heat transfer performance of the present convex fin is much better than the slit fin studied in [8].

Come here the comprehensive heat transfer performance of the studied convex-fin is evaluated. It is well-known that the enhancement techniques for air-gas are always accompanied by an increase in pressure drop, and often the ratio of pressure drop increase is larger than the increase of heat transfer rate. Thus it is extremely important to determine whether the enhancement technique is economically accepted or not compared with the reference surface. Fan et al. [36] proposed a performance evaluation plot to assess the performance of the enhanced surface based on a referenced surface. The details of the evaluation plot can be found in [36]. For the simplicity of presentation, only a brief introduction is presented below.

Assuming that for the reference surface the correlated equations of the friction factor and Nusselt number are as follows:

$$f_o(Re) = c_1 Re^{m_1} \tag{25}$$

$$Nu_o(Re) = c_2 Re^{m_2} \tag{26}$$

Then, the ratio of enhanced heat transfer rate over that of the referenced structure Q_e/Q_o can be expressed as follows:

$$C_{Q,i} = \frac{(Nu_e/Nu_o)_{Re}}{(f_e/f_o)_{Re}^{k_i}} \quad (i = P, \Delta p, V) \tag{27}$$

For identical pumping power constraint (i = *P*), the exponent $k_P = \frac{m_2}{3+m_1}$; for identical pressure drop constraint (i = Δp), $k_{\Delta p} = \frac{m_2}{2+m_1}$ and for identical flow rate constraint (i = *V*), $k_v = 1.0$.

If we set $\ln(Nu_e/Nu_o)_{\mathrm{Re}}$, $\ln(f_e/f_o)_{\mathrm{Re}}$ as the ordinate and abscissa, respectively, the logarithm of Eq. (27) displays as a straight line in the coordinate system. Setting $C_{Q,i} = 1$ as the origin of the coordinate, we can get a plot with three straight lines as shown in Fig. 14. The three lines divide the plot into four regions and the number of the regions (1, 2, 3 and 4) is shown in the figure. Any test data for enhancement study can be represented by a working point in this figure. If the working point is located in Region 1 the heat transfer is deteriorated based on the pumping power consumption. In Region 2 the heat transfer rate is enhanced based on the identical pumping power consumption (identical pumping power constraint). In Region 3 the heat transfer is enhanced based on the identical pressure drop constraint. Finally in Region 4 the increase of heat transfer rate is greater than that of the increase of friction

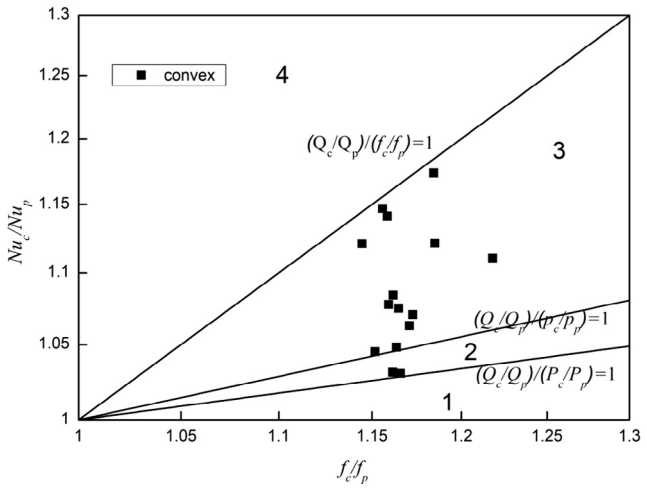

Fig. 14. Performance evaluation plot of convex-fin with plain-fin serving as reference.

factor under the same flow rate (identical flow rate constraint). It is obvious that any enhanced technique with its working point located in Region 1 is not accepted at least from energy-saving point of view, and that with its working point in Region 4 is the best.

The performance evaluation results of convex-fin with plain-fin as a reference are shown in Fig. 14. It can be seen from the figure that for all the test cases the convex-fin can enhance heat transfer at the constraint of identical pumping power, and for most cases it can enhance heat transfer at the identical pressure drop. This is very meaningful for heat transfer enhancement of air-cooler in compressor since as indicated above pressure drop is the major concern in designing an air-cooler in compressor system.

5. Conclusion

In this paper, an experimental investigation on heat transfer and friction characteristics of a new kind of enhanced surface is performed. Compared with conventional slit fin surface where the mouths of the slits are normal to flow direction, the major feature of this structure is that four convex-strips are around each tube, hence the four mouths are also around each tube. A plain-fin heat exchanger with the same dimension is also tested for comparison. The major findings are as follows.

The airside *Nu* number of the convex-fin sample is higher than that of the plain-fin sample. The Nusselt number ratio between convex-fin and plain-fin samples varies from 1.2 to 1.05 with the Reynolds number increase from 3000 to 15,000. In the test range, the Nusselt number may be well-correlated by a power law equation. The airside friction factor of convex-fin sample is higher than that of the plain-fin sample. The friction factor of the convex-fin sample is about 16% larger than that of the plain-fin sample. The correlations for plain fin proposed by Wang et al. can be applied to the plain fin-and-tube surface studied in this paper, even though tube diameter and tube row numbers are outside their data range. The correlation for heat transfer proposed by Nakayama and Xu can well predict the *j* factor of our new convex fin with proposed selection of two slit parameters (S_w and S_l). The friction factor of convex fin is much smaller than that of the slit fin studied by Nakayama and Xu. Compared with the plain fin, convex fin can always enhance heat transfer under the same pumping power condition. Most of the test data can get better heat transfer performance under the same pressure drop. Within the working velocity range of air mid-cooler in convectional compressor system, the tested convex fin surface is recommended to be applied to get better heat transfer performance in airside.

Acknowledgment

This study is supported by the National Key Basic Research Program of China (973 Program) (2013CB228304) and the 111 Project (B16038).

Appendix A. Measurement conditions and results

Run No.	G (kg/s)	Re	T_{in} (°C)	T_{out} (°C)	Q (W)	Δp (Pa)	η
Convex-fin							
1	0.1770	3438	14.11	106.19	16421.1	245.0	0.88
2	0.2168	4220	15.07	105.68	19679.8	323.4	0.86
3	0.2497	4840	14.85	107.21	23044.0	416.5	0.85
4	0.2872	5585	16.12	106.28	25783.5	509.6	0.84
5	0.3275	6397	16.48	104.78	28542.2	622.3	0.84
6	0.3630	7102	16.17	104.20	31720.4	744.8	0.83
7	0.4012	7875	16.48	103.07	34548.7	872.2	0.83
8	0.4383	8619	16.03	102.39	37757.3	1009.4	0.82
9	0.4769	9387	16.63	102.21	40843.0	1166.2	0.81
10	0.5216	10,305	17.00	101.07	43679.9	1323.0	0.81
11	0.5587	11,060	15.99	100.11	47,056.1	1489.6	0.80
12	0.5966	11,832	16.90	99.77	49698.5	1656.2	0.80
13	0.6355	12,613	16.86	99.55	52968.7	1842.4	0.79
14	0.6752	13,412	16.71	99.28	56308.3	2038.4	0.78
15	0.7946	15,926	16.15	96.03	63450.5	2665.6	0.77
Plain-fin							
1	0.1953	3799	13.67	105.52	17814.2	235.2	0.88
2	0.2321	4517	12.09	104.79	21602.2	313.6	0.87
3	0.3074	6025	12.77	102.57	28042.7	490.0	0.86
4	0.3904	7663	14.82	102.70	34239.2	705.6	0.84
5	0.4284	8420	15.24	102.42	37437.9	828.1	0.83
6	0.4691	9257	13.24	100.38	41065.7	950.6	0.83
7	0.5095	10,065	14.95	100.64	44478.9	1102.5	0.82
8	0.5479	10,869	15.27	99.27	46470.7	1244.6	0.82
9	0.5515	10,904	13.31	99.88	48611.5	1244.6	0.81
10	0.5941	11,786	15.24	99.27	50,249.0	1401.4	0.81
11	0.6336	12,592	15.22	98.72	53,262.5	1568.0	0.80
12	0.6382	12,713	13.40	97.36	54,015.2	1577.8	0.80
13	0.6745	13,455	15.00	97.42	56033.3	1734.6	0.79
14	0.7220	14,419	12.92	96.45	60475.5	1940.4	0.78
15	0.7603	15,237	14.78	95.85	62265.6	2116.8	0.78

References

[1] C.C. Wang, K.Y. Chi, Heat transfer and friction characteristics of plain fin-and-tube heat exchangers, Part I: New experimental data, Int. J. Heat Mass Transfer 43 (2000) 2681–2691.

[2] C.C. Wang, K.Y. Chi, C.J. Chang, Heat transfer and friction characteristics of plain fin-and-tube heat exchanger, Part II: Correlation, Int. J. Heat Mass Transfer 43 (2000) 2693–2700.

[3] Y.L. He, W.Q. Tao, F.Q. Song, Z.G. Qu, Three-dimensional numerical study of heat transfer characteristics of plain plate fin-and-tube heat exchangers from view point of field synergy principle, Int. J Heat Fluid Flow 26 (2005) 459–473.

[4] C.C. Wang, W.L. Fu, C.T. Chang, Heat transfer and friction characteristics of typical wavy fin-and-tube heat exchangers, Exp. Thermal Fluid Science 14 (1997) 174–186.

[5] Y.B. Tao, Y.L. He, Z.G. Wu, W.Q. Tao, Three-dimensional numerical study and field synergy principle analysis of wavy fin heat exchangers with elliptic tubes, Int. J Heat Fluid Flow 28 (2007) 1531–1544.

[6] Y.B. Tao, Y.L. He, J. Huang, W.Q. Tao, Numerical study of local heat transfer coefficient and fin efficiency of wavy fin-and-tube heat exchangers, Int. J Thermal Sciences 46 (2007) 768–778.

[7] Y.B. Tao, Y.L. He, J. Huang, W.Q. Tao, Three-dimensional numerical study of wavy fin-and-tube heat exchangers and field synergy principle analysis, Int. J. Heat Mass Transfer 50 (2007) 1163–1175.

[8] W. Nakayama, L.P. Xu, Enhanced fins for air-cooled heat exchangers-heat transfer and friction correlations, in: 1st ASME/JSME Therm. Engineering Joint Conference 1, 1983, pp. 495–502.

[9] C.C. Wang, C.H. Lee, C.T. Chang, S.P. Lin, Heat transfer and friction correlation for compact louvered fin-and tube heat exchangers, Int. J. Heat Mass Transfer 42 (1999) 1945–1956.

[10] J.Y. Yun, K.S. Lee, Investigation of heat transfer characteristics on various kinds of fin-and-tube heat exchangers with interrupted surfaces, Int. J. Heat Mass Transfer 42 (1999) 2375–2385.

[11] H. Kang, M.H. Kim, Effect of strip location on the air-side pressure drop and heat transfer in strip fin-and-tube exchanger, Int. J. Ref. 22 (1999) 302–312.

[12] G. Lozza, U. Merlo, An experimental investigation of heat transfer and friction losses of interrupted and wavy fins for fin-and-tube heat exchangers, Int. J. Refrigerat. 24 (2001) 409–416.

[13] Y.P. Cheng, Z.G. Qu, W.Q. Tao, Y.L. He, Numerical design of efficient slotted fin surface based on the field synergy principle, Numer. Heat Transfer, Part A 45 (6) (2004) 517–538.

[14] Z.G. Qu, W.Q. Tao, Y.L. He, Three-dimensional numerical simulation on laminar heat transfer and fluid flow characteristics of strip fin surface with x-arrangement of strips, ASME J. Heat Transfer 126 (2004) 697–707.

[15] J.J. Zhou, W.Q. Tao, Three dimensional numerical simulation and analysis of the airside performance of slotted fin surfaces with radial strips, Eng. Comput. 22 (2005) 940–957.

[16] W.Q. Tao, W.W. Jin, Y.L. He, Optimum design of two-row slotted fin surface with X-shape strip arrangement positioned by "front course and rear dense" principle, Part I: Physical/mathematical models and numerical methods, Numer. Heat Transfer, Part A 50 (2006) 731–749.

[17] W.W. Jin, Y.L. He, Z.G. Qu, C.C. Zhang, W.Q. Tao, Optimum design of two-row slotted fin surface with X-shape strip arrangement positioned by "front coarse and rear dense" principle, Part II: Results and discussion, Numerical Heat Transfer, Part A 50 (2006) 751–771.

[18] W.Q. Tao, Y.P. Cheng, T.S. Lee, The influence of strip location on the pressure drop and heat transfer performance of a slotted fin, Numerical Heat Transfer, Part A 52 (2007) 463–480.

[19] N.H. Kim, H. Cho, An experimental investigation of the air-side performance of fin-and-tube heat exchangers having slit fins, J. Enhanced Heat Transfer 22 (2015) 67–88.

[20] M. Fiebig, A. Valencia, N.K. Mitra, Wing-type vortex generators for fin-and-tube heat exchangers, Exp. Therm. Fluid Sci. 7 (4) (1993) 287–295.

[21] A.M. Jacobi, R.K. Shah, Heat transfer surface enhancement through the use of longitudinal vortices: a review of recent progress, Exp. Therm. Fluid Sci. 11 (3) (1995) 295–309.

[22] A. Joardar, A.M. Jacobi, A numerical study of flow and heat transfer enhancement using an array of delta-winglet vortex generators in a fin-and-tube heat exchanger, ASMEJ Heat Transfer 129 (9) (2007) 1156–1167.

[23] J.M. Wu, W.Q. Tao, Investigation on laminar convection heat transfer in fin-and-tube heat exchanger in aligned arrangement with longitudinal vortex generator from the viewpoint of field synergy principle, J. Appl. Thermal. Eng. 27 (14–15) (2007) 2609–2617.

[24] L.T. Tian, Y.L. He, Y.G. Lei, W.Q. Tao, Numerical study of fluid flow and heat transfer in a flat-plate channel with longitudinal vortex generators by applying field synergy principle analysis, Int. Commun. Heat Mass Transfer 36 (2) (2009) 111–120.

[25] Y.L. He, Y.W. Zhang, Advances and outlooks of heat transfer enhancement by longitudinal vortex generators, Edited by Ephraim M. Sparrow, Young I. Cho, John P. Abraham and John M. Gorman, Adv. Heat Transfer 44 (2012) 119–185, chap. 2.

[26] M.J. Li, W.J. Zhou, J.F. Zhang, J.F. Fan, Y.L. He, W.Q. Tao, Heat transfer and pressure performance of a plain fin with radiantly arranged winglets around each tube in fin-and-tube heat transfer surface, Int. J. Mass Heat Transfer 70 (2014) 734–744.

[27] S.M. Yang, W.Q. Tao, Heat Transfer, fourth ed., Higher Education Press, Beijing, China, 2006.

[28] T.E. Schmidt, Heat transfer calculations for extended surfaces, J. ASRE, Refrig. Eng. 4 (1949) 351–357.

[29] R.J. Moffat, Describing the uncertainties in experimental results, Exp. Thermal Fluid Sci. 1 (1988) 3–17.

[30] J.R. Taylor, An Introduction to Error Analysis: the Study of Uncertainties in Physical Measurements, University Science Books, Mill Valley, California, 1982.

[31] B. Cheng, W.Q. Tao, Experimental study of R-152a film condensation on single horizontal smooth tube and enhanced tubes, ASME J. Heat Transfer 116 (1994) 266–270.

[32] D.C. Zhang, Experimental and numerical investigation of refrigerant condensation and boiling heat transfer characteristics on doubly-enhanced tubes, Dissertation, School of Energy and Power engineering, Xi'an Jiaotong University, 2007

[33] W.T. Ji, C.Y. Zhao, D.C. Zhang, Y.L. He, W.Q. Tao, Influence of condensate inundation on heat transfer of R134a condensing on three dimensional enhanced tubes and integral-fin tubes with high fin density, Appl. Therm. Eng. 38 (2012) 151–159.

[34] W.T. Ji, C.Y. Zhao, D.C. Zhang, Y.L. He, W.Q. Tao, Condensation of R134a outside single horizontal titanium, cupronickel 4 (B10 and B30), stainless steel and copper tubes, Int. J. Heat Mass Transfer 77 (2014) 194–201.

[35] A. Zukauskas, Convection heat transfer in cross flow, in: J.P. Hartnett, T.F. Irvine (Eds.), Advances in Heat Transfer, 8, Academic Press, New York, 1972, pp. 93–106.

[36] J.F. Fan, W.K. Ding, J.F. Zhang, Y.L. He, W.Q. Tao, A performance evaluation plot of enhanced heat transfer techniques oriented for energy-saving, Int. J. Heat Mass Transfer 52 (2009) 33–44.